Biosensors and Bioelectronics 69 (2015) 287–293

Contents lists available at ScienceDirect

Biosensors and Bioelectronics

journal homepage: www.elsevier.com/locate/bios

An electrochemical biosensor based on DNA tetrahedron/graphene composite film for highly sensitive detection of NADH

Zonglin Li [a], Wenqiong Su [b], Shuopeng Liu [a], Xianting Ding [a,*]

[a] Med-x Research Institute, Shanghai Jiao Tong University, Shanghai 200240, PR China
[b] School of Chemistry and Chemical Engineering, State Key Laboratory Metal Matrix Composites, Shanghai Jiao Tong University, Shanghai, 200240, PR China

ARTICLE INFO

Article history:
Received 26 November 2014
Received in revised form
7 February 2015
Accepted 19 February 2015
Available online 2 March 2015

Keywords:
NADH detection
Electrochemical
Gold nanoparticles
DNA tetrahedron
Graphene

ABSTRACT

Dihydronicotinamide adenine dinucleotide (NADH) is a major biomarker correlated with lethal diseases such as cancers and bacterial infection. Herein, we report a graphene-DNA tetrahedron-gold nanoparticle modified gold disk electrode for highly sensitive NADH detection. By assembling the DNA tetrahedron/graphene composite film on the gold disk electrode surface which prior harnessed electrochemical deposition of gold nanoparticles to enhance the effective surface area, the oxidation potential of NADH was substantially decreased to 0.28 V (vs. Ag/AgCl) and surface fouling effects were successfully eliminated. Furthermore, the lower detection limit of NADH by the presented platform was reduced down to 1 fM, with an upper limit of 10 pM. Both the regeneration and selectivity of composite film-modified electrode are investigated and proved to be robust. The novel sensor developed here could serve as a highly sensitive probe for NADH detection, which would further benefit the field of NADH related disease diagnostics.

1. Introduction

Dihydronicotinamide adenine dinucleotide (NADH), as an important coenzyme for almost all biological metabolic processes (Ying, 2008), is correlated to a variety of diseases including breast cancer (Yu and Heikal, 2009) and Parkinson's disease (Vrecko et al., 1997). NADH is also highly correlated to cell failure and death (Alano et al., 2004; Virag and Szabo, 2002; Ying, 2008). Besides, the monomer number of some kinds of bacteria is positive correlated with the concentration of NADH since the free NADH concentration is constant in bacterial monomer cell (Kasimova et al., 2006; Wimpenny and Firth, 1972). Therefore, to detect NADH concentration level with high sensitivity can provide a novel approach for the early diagnosis of these related diseases.

Conventionally, NADH detection methods mainly include high performance liquid chromatography (HPLC) (Yates and Merrill, 2005), enzymatic cycling method (Bernofsky and Swan, 1973) and fluorescence method (Renault et al., 1982). Yet, HPLC is limited by its low sensitivity (Nangreave et al., 2010), enzymatic cycling method is time-consuming (Bernofsky and Swan, 1973), while fluorescence method is expensive and inconvenient (Renault et al., 1982; Yu and Heikal, 2009). Taking advantage of NADH redox properties, in this paper, a classical "three-electrode" configuration is applied to achieve high-sensitivity detection of NADH by electrochemical method.

Problem inherent to electrochemical method is the large oxidation potential encountered for NADH oxidation, which may cause surface fouling on the working electrode (Blaedel and Jenkins, 1975; Moiroux and Elving, 1978; Samec and Elving, 1983). With the development of nanotechnology, nanomaterials such as carbon nanotubes (Musameh et al., 2002), carbon fiber (Wu et al., 2007) and polymers (Manesh et al., 2008), have been used to decrease the oxidation potential successfully. In comparison with carbon nanomaterials, with the advantages of high specific surface area, low cost and ease of processing and safety (Segal, 2009), graphene receives much popularity these days. Just like a warehouse of electrons, graphene has remarkably high electron mobility at room temperature (Geim and Novoselov, 2007), which may benefit the reducing of NADH oxidation potential. The biological applications of graphene for NADH detection have already been explored by many researchers. For instance, Li et al. created a sensitive NADH biosensor based on the combination of graphene and gold nanorods which decreased the oxidation potential of NADH to 0.4 V (Li et al., 2013b). Meanwhile, a nanocomposite film consisting of electroreduced graphene oxide and polythionine was also used to construct an amperometric biosensor on the surface of a glassy carbon electrode (GCE) and to determinate NADH at 0.4 V (Li et al., 2013c). Shan et al. modified a GCE with ionic liquid-functionalized graphene (IL-graphene) to decrease the oxidation potential of NADH to 0.33 V (Shan et al., 2010). With the assistance

* Corresponding author.
E-mail address: dingxianting@sjtu.edu.cn (X. Ding).

http://dx.doi.org/10.1016/j.bios.2015.02.031
0956-5663/

of Fe_3O_4 magnetic nanoparticles/reduced graphene oxide nanosheets, the oxidation potential of NADH was even decreased to 0.05 V (Teymourian et al., 2013). Therefore, it is noted that graphene fragments of excellent electric conductivity may be helpful to decrease the oxidation potential of NADH (Shao et al., 2010). The problem is that, through the strong van der Waals interaction and π–π stacking, graphene fragments tend to form irreversible agglomerates easily (Li et al., 2008), which may cause adverse effects for the detection system. Hence it is significant to prevent the aggregation via particular modification of the electrode surface.

Inspired by the DNA origami technology, constructing scaffolds to insert graphene fragments may not only prevent the aggregation but also increase the effective contact area. DNA origami has been researched for construction of nanoscale objects for nearly 30 years (Nangreave et al., 2010), which has been used to study single-molecule chemical reactions (Voigt et al., 2010), to assemble water-soluble probe tiles for label-free RNA hybridization (Ke et al., 2008), to organize a variety of relevant molecules including carbon nanotubes (Maune et al., 2010) and metal nanoparticles (Ding et al., 2010; Pal et al., 2010), and to probe distance-dependent multivalent ligand–protein binding effects (Rinker et al., 2008). Scaffolded DNA origami technology has been developed from two-dimensional (2D) structures to three-dimensional (3D) objects (Nangreave et al., 2010), and as one of them, DNA tetrahedrons, which are used to serve as scaffolds in this paper, receives much popularity these days. DNA tetrahedrons were constructed from the self-assembling of three thiolated 55-base oligonucleotides and one 55-base oligonucleotide (Pei et al., 2010) 3D-structured probes for DNA detection (Pei et al., 2010) due to their advantages of easily controlling the orientation and density, and good passivation of the modified surface (Pei et al., 2013). And then, by using the self-assembled DNA tetrahedron nanostructures as the capture probes, Wen et al. reported an electrochemical biosensor to detect cocaine with a remarkably low detection limit of 33 nM. (Wen et al., 2011), while the DNA tetrahedron nanostructures were also applied in the fields of smart drug delivery nanocarriers (Li et al., 2013a) and intracellular logic sensors (Pei et al., 2012).

With unique properties such as great conductivity, electrochemical stability, biological compatibility and enhanced catalysis, gold nanoparticles were used for signal amplification in numerous biosensing applications (Cao et al., 2011). As for NADH detection, carbon-supported gold nanoparticle (AuNP/C) modified electrode showed remarkable properties than glassy carbon (GC), carbon (C) and gold nanoparticles (AuNP) towards NADH oxidation (Shim et al., 2013). Tiwari and Gupta constructed a newly gold nanoparticles/neutral red/MWCNTs modified glassy carbon electrode to detect NADH with better adhesion over the electrode surface and good stability (Tiwari and Gupta, 2014). Because of the three thiol function groups at the bottom of the 'pyramid', the DNA tetrahedrons can anchor strongly and readily on gold and/or gold nanoparticle surface (Pei et al., 2013). In order to further increase the surface area and the electron mobility, the gold nanoparticles were introduced in this work.

Therefore, in this paper, a graphene-DNA tetrahedron-gold nanoparticle modified gold disk electrode was prepared and its electrochemical sensing behaviors for NADH detection were investigated firstly. Compared with previously reported sensors, as for NADH detection, this newly developed electrode exhibited great performance for decreasing of NADH oxidation potential. Both the regeneration and selectivity of composite film-modified electrode were explored and proved to be robust. The novel sensor developed could serve as a highly sensitive device for NADH concentration detection, which would further benefit the field of NADH related disease diagnostics.

2. Experimental

2.1. Reagents and materials

DNA was obtained from Takara (Dalian, PRC), which is purified by HPLC. XF005-4 import amino-graphene TEPA (four amino) was brought from XFNANO Materials Tech CO., Ltd (Nanjing, PRC). NADH was obtained from Acros, USA. All other reagents and materials were of analytical grade or better. By mixing the solutions of NaCl (Acros, USA), KCl (Vetec, USA), Na_2HPO_4 (Acros, USA) and KH_2PO_4 (Adamas, PRC), phosphate buffer solution (PBS, 0.1 M, pH 7.4) was prepared. TE buffer containing the aqueous solutions of 10 mM Tris (99.8%, Acros, USA) and 1 mM EDTA (99%, Acros, USA) and TM buffer, the mixture of 20 mM Tris and 50 mM $MgCl_2 \cdot 6H_2O$ (99%, Adamas, PRC) were adjusted at pH 8 and applied to construct DNA tetrahedrons. Meanwhile, 30 mM Tris (2-carboxyethyl) phosphine (TCEP, Acros, USA) solution was prepared with TM buffer. Cell lysis was mixed by 0.04% Triton-X100, 2 mM HEPES, 0.2 mM dithiothreitol, 0.01% bovine serum albumin and 0.1% phenol red (pH 7.5). Milli-Q water was obtained from Milli-Q Academic systerm (Millipore, USA) and used to prepare all aqueous solutions.

2.2. Apparatus and measurements

Electrochemical measurements were carried out by CHI660E electrochemical workstation (CH Instruments, USA). A conventional three-electrode configuration was established with a gold disk electrode (diameter: 2 mm) as the working electrode, a platinum sheet as the counter electrode, and a Ag/AgCl electrode (c (KCl)=3 mol/L) as the reference electrode. The gold printed electrodes (DRP-220AT, DropSens, Spain) were adopted as gold plate electrodes for the Atomic force microscope (AFM, Bioscope, Bruker, Germany) test.

2.3. Construction of DNA tetrahedron

Construction of DNA tetrahedron was according to the protocol published before (Pei et al., 2010) with a little modification. Four well-designed DNA strands applied in this research were listed as follows:

Strand A:5′-ACATTCCTAAGTCTGAAACATTACAGCTTGCTACACG AGAAGAGCCGCCATAGTA-3′

Strand B:5′-HS-C_6-TATCACCAGGCAGTTGACAGTGTAGCAAGCT GTAATAGATGCGAGGGTCCAATAC-3′

Strand C:5′-HS-C_6-TCAACTGCCTGGTGATAAAACGACACTACGTG GGAATCTACTATGGCGGCTCTTC-3′

Strand D:5′-HS-C_6-TTCAGACTTAGGAATGTGCTTCCCACGTAGTGT CGTTTGTATTGGACCCTCGCAT-3′

16 groups of the DNA mixture solutions (the formulas of them were shown in Table S1 in supporting information) were obtained and vibrated for 2 min, incubated at 95 °C for 2 min and cooled down to 4 °C quickly. Then DNA agarose gel electrophoresis was used to explore the result of DNA tetrahedron construction.

2.4. Dispersion of graphene fragments

0.25 mg/mL amino-graphene solution was ultrasonic-concussed (DH95-IIDN, Dihao, PRC) for several hours and then centrifuged for 20 min at 3000 r/min. The supernatant was obtained to have Transmission electron microscopy (TEM) test (JEM-2010 transmission electron microscopy, USA) operating at 120 kV.

2.5. Fabrication of the developed biosensor

Gold disk electrodes were polished by a MP-1B polishing and

burnishing machine (Wanheng, Shanghai) with 0.05 μm alumina slurry, soaked in Piranha Solution (mixed with 98% H_2SO_4 and 35% H_2O_2,v/v 3:1) for 10 min then washed ultrasonically in water and acetonitrile for 5 min each.

Gold nanoparticles were electrochemically deposited on the well-polished gold disk electrode in 0.5 M H_2SO_4 aqueous solution containing 10 mM $HAuCl_4$ at −0.2 V for 60 s (Su et al., 2013). Then it was immersed in 250 nM DNA tetrahedron solution for 3 h to establish a firm self-assembled monolayer. After raised with Milli-Q water, 10 μL of the ultrasonic-concussed amino-graphene solution was dropped on the DNA tetrahedron-modified gold disk electrode surface. After a while, the graphene-modified electrode was raised with Milli-Q water. The last two steps were repeated several times to finally construct the graphene-DNA tetrahedron-gold nanoparticle modified gold disk electrode. AFM was used to prove the construction of the composite film modified electrode. The schematic structure of the newly graphene-DNA tetrahedron-gold nanoparticle modified gold disk electrode was shown in Scheme 1.

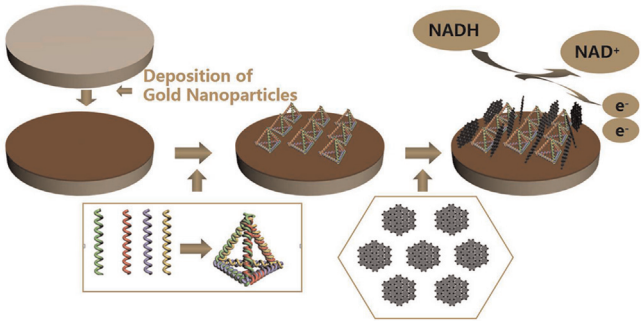

Scheme 1. Construction process for the graphene-DNA tetrahedron-gold nanoparticle modified gold disk electrode.

2.6. Detection of NADH

The newly developed graphene-DNA tetrahedron-gold nanoparticle modified gold disk electrode was applied in PBS solutions containing NADH of different concentrations. Differential pulse voltammetry (DPV) was conducted at a certain voltage range to explore the electrochemical response of the composite film-modified electrode to NADH. As for regeneration, DPV curve in 1 pM NADH/PBS solution of the composite film-modified electrode was obtained firstly. Then the used composite film-modified electrode was rinsed with 0.01 M PBS (pH 7.4) thoroughly to remove the NADH molecules which were potentially adsorbed on the surface of the composite film-modified electrode. The regenerated composite film-modified electrode was applied to electrochemical detection in the fresh PBS solution containing 1 pM NADH by DPV. Additionally, prepared cell lysis was diluted 50 times and used to compound 1 pM NADH solution to simulate cellular environment. DPV curve of the composite film-modified electrode immersed in this cell lysis was also recorded to testify the selectivity of the developed NADH biosensor.

3. Results and discussion

3.1. Construction of DNA tetrahedron

To serve as scaffolds for graphene fragments, DNA tetrahedrons were investigated and constructed firstly. DNA agarose gel electrophoresis was introduced to prove the successful assembling of the four well-designed DNA strands following the principle of complementary base pairing. DNA agarose gel electrophoresis, as a method for separation and analysis of DNA molecules, can estimate the size of DNA molecules since small ones move faster and migrate farther than large ones due to the bigger hindrance of larger molecules through the pores of the agarose gel. The results

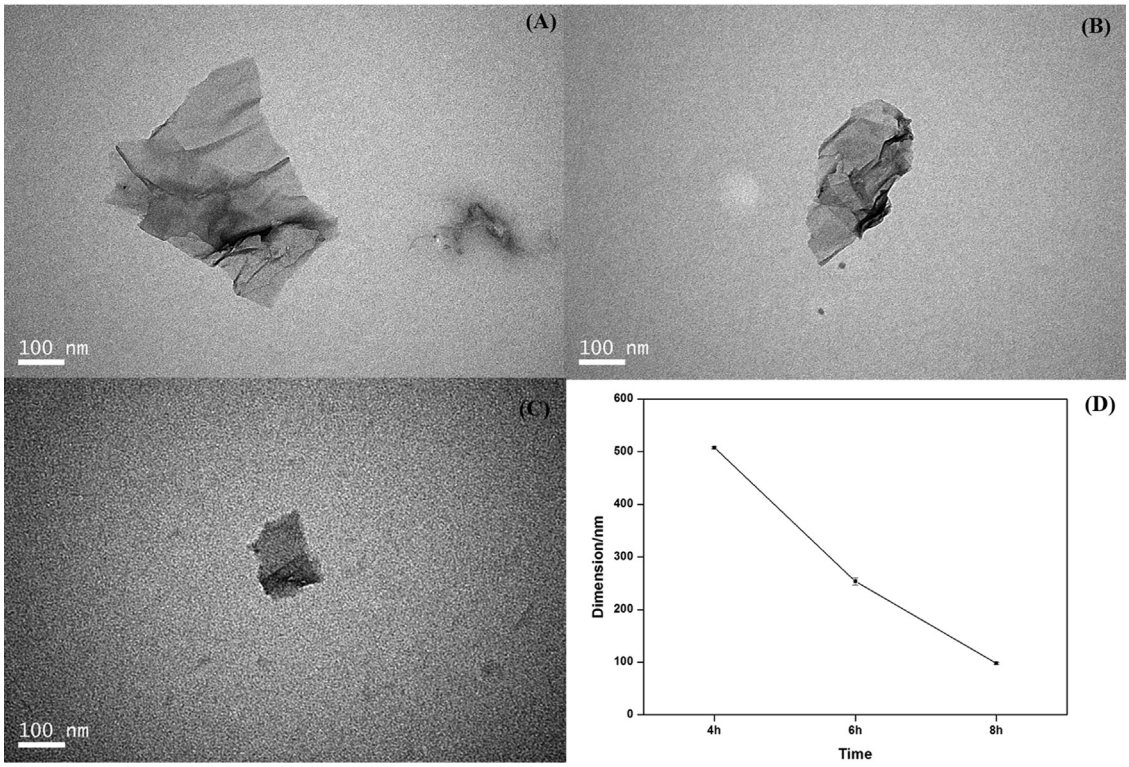

Fig. 1. (A) TEM image of amino-graphene fragment in group A. (B) TEM image of amino-graphene fragment in group B. (C) TEM image of amino-graphene fragment in group C. (D) Statistic results of amino-graphene fragments' average dimension of group A, B and C.

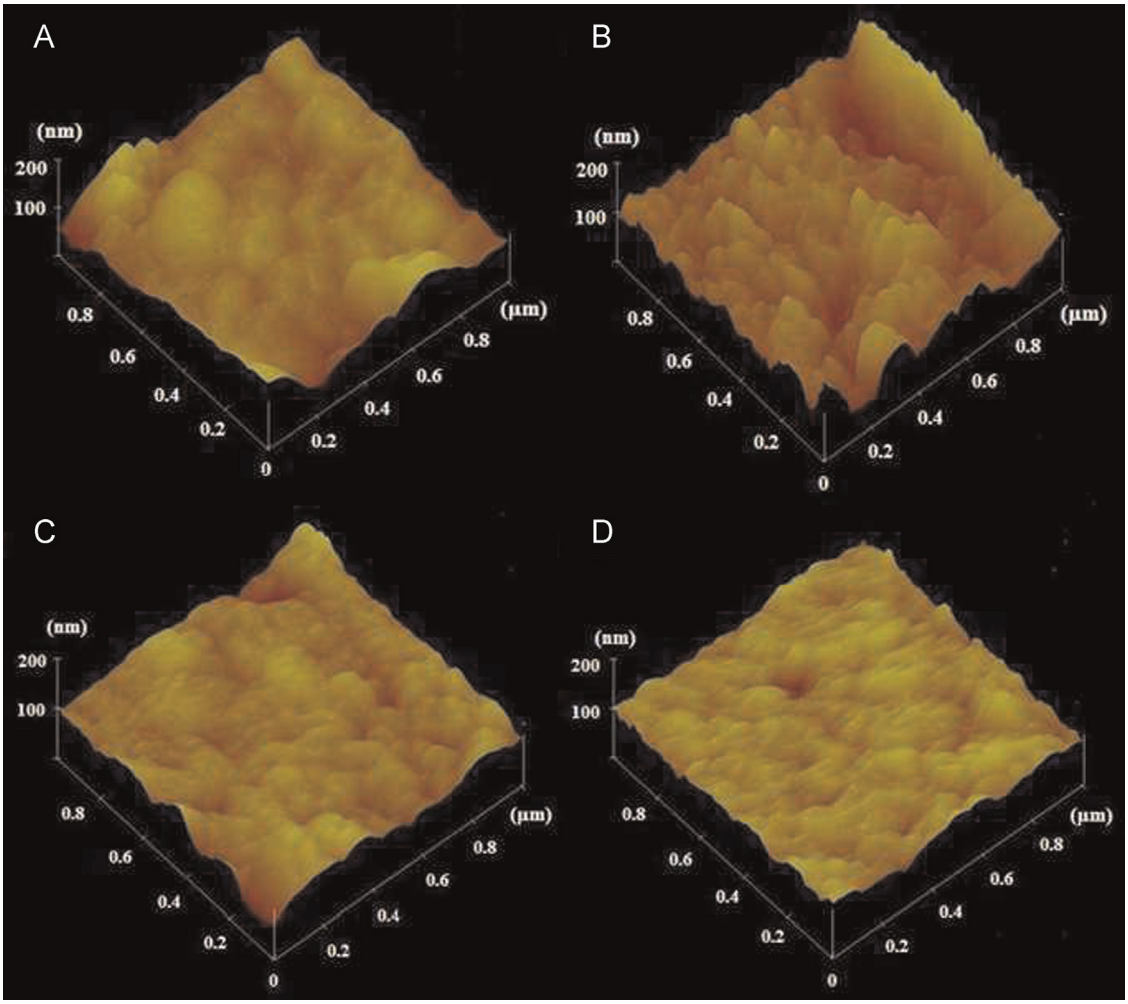

Fig. 2. AFM images of the bare gold electrode (A) modified with gold nanoparticles (B), gold nanoparticles/DNA tetrahedrons (C) and gold nanoparticles/DNA tetrahedrons/graphene (D).

were shown in Fig S1 in supporting information. 50 bp DNA Ladder Marker was on the left to be scale. Control studies showed that the DNA tetrahedrons (line o and p, close to 200 bp) moved more slowly than either the single DNA strand (line a, b, c, d, close to 50 bp) or any other combinations lacking one (line k, l, m, n, close to 150 bp) or two strands (line e, f, g, h, i, j, close to 100 bp), confirming the fact that the DNA nanostructures were assembled successfully.

3.2. Dispersion of graphene fragments

Appropriate graphene fragments were needed to cooperate with well-constructed DNA tetrahedrons. Therefore, three experiment conditions of graphene dispersion were explored before combination of graphene fragments on the electrode. 0.25 mg/mL amino-graphene solution of group A was ultrasonically dispersed for 4 h, while group B for 6 h and group C for 8 h. Fig.1(A–C) were the representative TEM images from each group. Fig.1D showed the tendency of average diameter of the amino-graphene fragments changing over ultrasonic time. As seen from Fig.1D, the longer the ultrasonic concussion lasted, the smaller the average diameter of amino-graphene fragments was. After ultrasonic concussion for 8 h, the mean diameter of the amino-graphene fragments was decreased to 100 nm, which was appropriate to cooperate with DNA tetrahedrons (Pei et al., 2010) to form the organic/inorganic composited film on gold disk electrode surface.

3.3. Characterization of the composite film modified gold disk electrodes

Self-assembled monolayers (SAMs) can serve as good platforms to build molecular level interface because of the high degree of order, diversity and good stability. With a strong affinity for thiol compounds, gold disk electrode usually serves as platform for SAMs (Li et al., 2010). Therefore, thiols were designed and modified at the terminals of B, C and D DNA strands to form the thiol-DNA tetrahedrons, which can anchor strongly and readily on gold surface (Pei et al., 2013). Meanwhile, the subsequent exposure of a pristine gold surface and the reliable removal of contaminants inherent on ambient surfaces sensitively affect the ability of fabricating high-quality self-assembled layers (Tkac and Davis, 2008). So the gold disk electrode needs to be well polished before the electrochemical deposition of gold nanoparticles. The electrochemical method was used to testify the well-polishment. The cyclic voltammograms from 0 to 1.5 V at 0.1 V/s in 1 M H_2SO_4 obtained at the well-polished bare gold electrode were shown in Fig S2 in supporting information. With the increasing numbers of scan cycles, the cyclic voltammetry curves gradually stabilized, and there was a broad anodic peak with peak potential of around 1.2 V and a single sharp reduction peak with peak potential between 0.9 and 1.0 V, which was consistent with the typical gold electrode cyclic voltammograms (Tkac and Davis, 2008), indicating that the gold disk electrode was correctly pretreated to composite

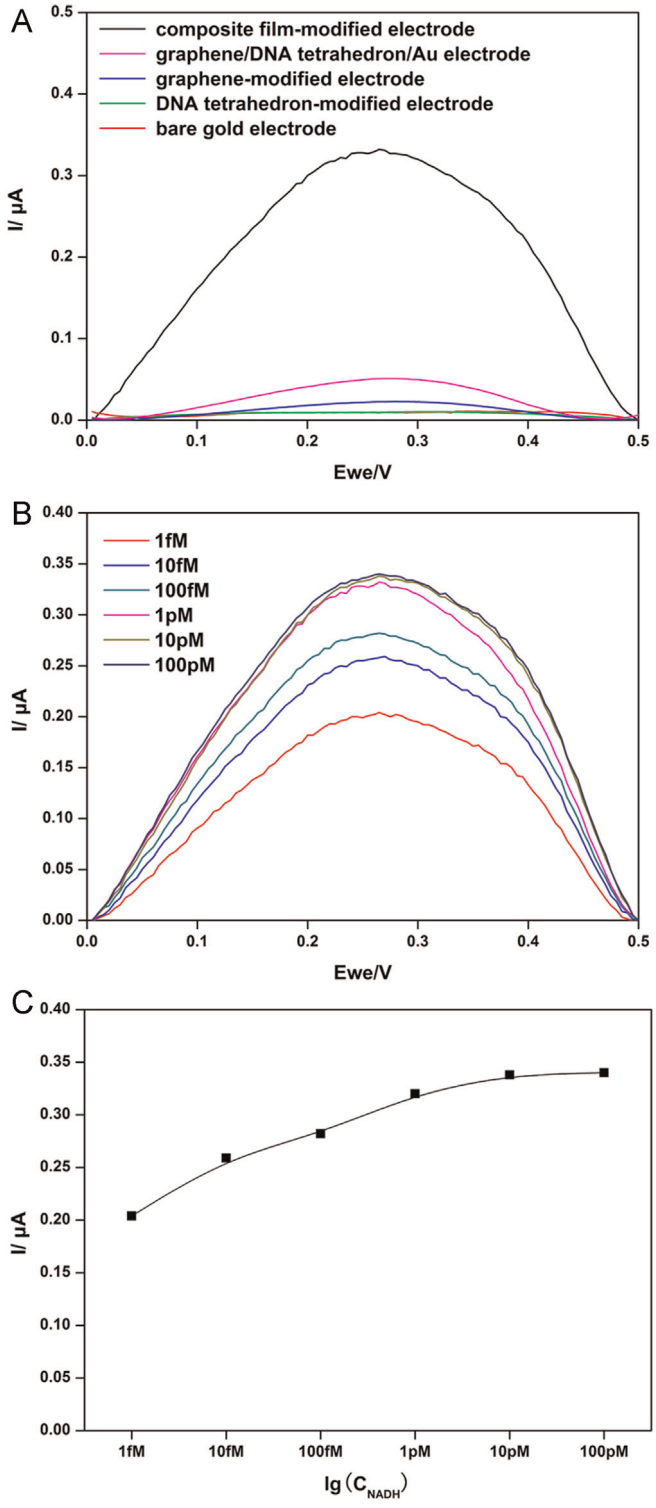

Fig. 3. (A) DPV curves of the bare gold disk electrode, graphene-modified gold disk electrode, DNA tetrahedron-modified gold disk electrode, graphene/DNA tetrahedron-modified gold disk electrode and the composite film-modified electrode in 1 pM NADH in PBS (pH 7.4) (B) DPV curves of the composite film-modified electrode detecting NADH of different concentrations (1 fM, 10 fM, 100 fM, 1 pM, 10 pM and 100 pM). (C) Amperometric response to NADH concentration.

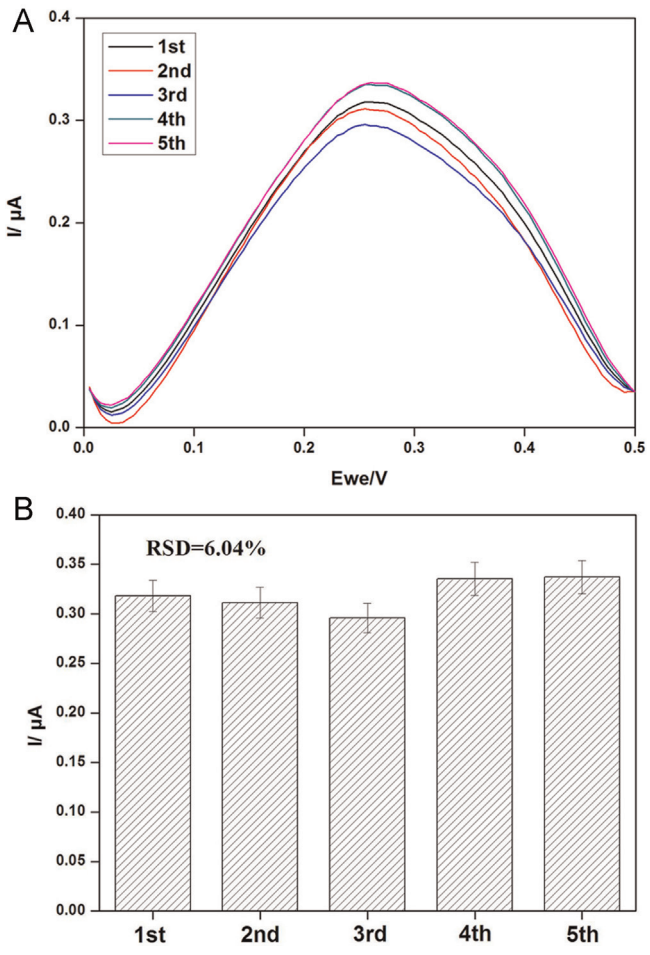

Fig. 4. (A) DPV curves of the successive five detection in 1 pM NADH/PBS solution with the reused composite film-modified electrode for regeneration investigation. (B) Histogram for the peak currents of successive five detection.

the rest materials.

Gold nanoparticles were deposited on the gold disk electrode through electrochemical method to increase the effective surface area and the electron mobility. The cyclic voltammograms from 0 to 1.5 V at 0.1 V/s in 1 M H_2SO_4 obtained at the well-polished bare gold electrode and the gold nanoparticle modified gold disk electrode were shown in Fig S3 in supporting information. The tremendous increase of both the anodic peak and the reduction peak indicated the successful deposition of gold nanoparticles. Then the well-constructed DNA tetrahedrons, served as scaffolds for graphene fragments, were self-assembled on the gold nanoparticle modified gold disk electrode through their three thiol ends.

Under the optimum conditions, the composite film-modified electrode was constructed as Scheme 1 shown and the fabrication process was investigated by AFM. As Fig.2A showed, a mean roughness of 42.5 nm was obtained from an original bare gold plate electrode. Fig.2B was the AFM image of the gold electrode after electrochemical deposition of gold nanoparticles, with the roughness of 65.2 nm. Fig.2C was obtained from the DNA tetrahedrons self-assembled gold nanoparticle-covered electrode, meanwhile the roughness was increased to 80.3 nm indicting the successful anchoring of DNA tetrahedrons on the gold disk electrode surface. After dropping amino-graphene solution on the modified gold disk electrode surface, the amino-graphene fragments were adsorbed on the DNA tetrahedron-assembled gold surface because of the interaction between electropositive amino-graphene fragments and electronegative DNA tetrahedrons. As for Fig.2D, the mean roughness of 81.5 nm was closed to 80.3 nm in Fig. 2C which demonstrated the fact that the amino-graphene fragments were inserted among DNA tetrahedrons rather than lying flat on the top of DNA tetrahedrons. Obviously, the graphene fragments of “standing” position showed more effective area than

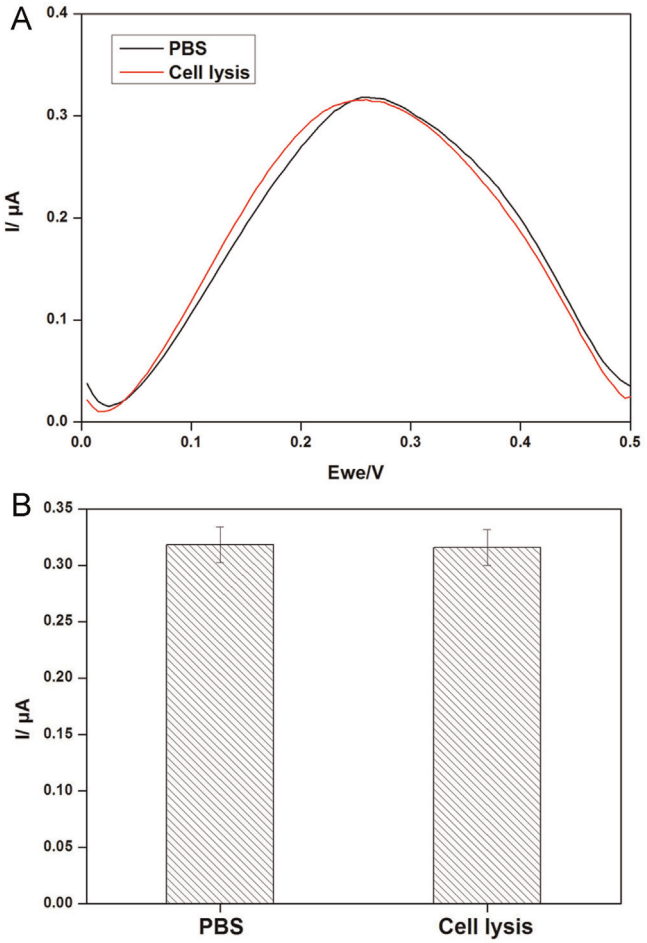

Fig. 5. (A) DPV curves of the composite film-modified electrode immersed in 1 pM NADH dissolved in 0.01 M PBS (pH 7.4) and cell lysis for selectivity test. (B) Histogram for the peak currents of the two different solution.

"lying down" ones, which probably offer more opportunity to adsorb and react with NADH molecules.

3.4. Electrochemical response of NADH detection with the developed biosensor

Since the composite film-modified electrode was demonstrated to be constructed successfully, it served as a newly constructed working electrode (vs. Ag/AgCl) to detect NADH through electrochemical method. Differential pulse voltammetry (DPV) was introduced to explore the electrochemical response of the composite film-modified electrode to NADH. Fig.3 A showed the DPV results obtained from bare, graphene-modified, DNA tetrahedron-modified and graphene/DNA tetrahedron-modified gold disk electrodes (all served as control studies) and the developed composite film-modified gold disk electrode in 1 pM NADH/PBS (0.1 M, pH 7.4) as electrolyte. Because of the cooperation of gold nanoparticles, DNA tetrahedrons and graphene fragments, there was an obvious oxidation peak of NADH at 0.28 V conducted with the composite film-modified electrode while there were less or no oxidation peaks aroused from the rest of electrodes invovled in the control experiments. Compared with the results reported with other graphene-modified electrodes, such as ionic liquid-functionalized graphene (IL-graphene) (0.33 V) (Shan et al., 2010), graphene-modified gold nanorods (0.4 V) (Li et al., 2013b) and electroreduced graphene oxide-polythionine nanocomposite film (0.4 V) (Li et al., 2013c), the NADH oxidation reaction occurred at a lower potential with the developed composited film-modified electrode.

The enhanced activity of graphene modified electrodes toward NADH oxidation may be attributed to the high density of the edge-plane-like defective sites among graphene fragments, which was further confirmed by Lin et al. (2009). It was reported that much of the catalytic activity and chemical reactivity of graphitic electrodes was at the surface defect sites, in particular edge-plane-like defect sites, which provided active sites for electron transfer to small biomolecules such as NADH (Banks et al., 2005). Pumera et al. proved that the carboxylic groups present in sp^2 carbon materials were formed at the edges and edge-like defects of graphene due to spontaneous oxidation in air and had the contribution to the NAD^+ adsorption (Pumera et al., 2009). Additionally, the DNA tetrahedrons serving as scaffolds could keep graphene fragments "standing" among them instead of lying down on the surface, which offered more opportunities for graphene fragments to adsorb and react with NADH molecules. The gold nanoparticles were involved to increase the effective surface area of gold electrode. Accordingly, the oxidation potential of NADH was decreased with the developed composite film-modified electrode. However, the recondite mechanisms still need more researches and investigations.

The freshly prepared graphene-DNA tetrahedron-gold nanoparticle modified gold disk electrode was applied to detect NADH at different concentrations by DPV from 0 to 0.5 V. Fig.3B showed the DPV results of the composite film-modified gold electrode conducted in NADH solutions of different concentration from 1 fM to 100 pM. The peak current was increased as the concentration of NADH solution increased. To be more precise, Fig.3C was plotted by using lg (C_{NADH}) as abscissa and the peak current as ordinate. As seen from Fig.3C, the lower detection limit of NADH by the composite film-modified electrode was reduced down to 1 fM, with a 10 pM upper limit. Compared to the detection limit of the graphene/nanostructures combined material mentioned above, such as graphene-Au nanorods nanocomposites (6.0 μM) (Li et al., 2013b), Fe_3O_4 magnetic nanoparticles/reduced graphene oxide nanosheets (0.4 μM) (Teymourian et al., 2013) and electroreduced graphene oxide-polythionine nanocomposite film (0.1 μM) (Li et al., 2013c), the graphene-DNA tetrahedron-gold nanoparticle modified gold disk electrode exhibited a much lower detection limit of NADH.

3.5. Regeneration and selectivity of the developed biosensor

The graphene-DNA tetrahedron-gold nanoparticle modified gold disk electrode can be easily regenerated by thoroughly rinsed with PBS to remove the potentially adsorbed NADH molecules. By successive five detection in 1 pM NADH/PBS solution, the reused composite film-modified gold electrode exhibited stable DPV response (Fig. 4A). As shown in Fig. 4B, the histogram of the detection peak current after regeneration was established with the RSD of 6.04% ($n=5$), indicating the regeneration possibility of the graphene-DNA tetrahedron-gold nanoparticle modified gold disk electrode.

The selective detection of NADH in simulative cellular environment was also investigated with the graphene-DNA tetrahedron-gold nanoparticle modified gold disk electrode. Cell lysis was diluted and used to prepare 1 pM NADH, mimicking cellular environment. Fig.5A showed the two overlapped DPV curves obtained from 1 pM NADH dissolved in PBS and cell lysis with the composite film-modified gold electrode. Fig. 5B showed the histogram of the DPV peak current. It is clear that there are almost no statistical differences between the two groups. Therefore, the newly constructed graphene-DNA tetrahedron-gold nanoparticle modified gold disk electrode was demonstrated to be feasible to selectively detect NADH in a simulative cellular environment.

4. Conclusion

A graphene-DNA tetrahedron-gold nanoparticle modified gold disk electrode for highly sensitive and stable low-potential amperometric detection of NADH has been explored and developed in this paper. The graphene-DNA tetrahedron-gold nanoparticle modified gold disk electrode remarkably decreases the oxidation voltage of NADH to 0.28 V and eliminates surface fouling effects. At the same time, the composite film-modified gold electrode reduced the lower limit of NADH detection to 1 fM, with an upper limit of 10 pM, which can achieve the purpose to detect NADH in low concentration range. The regeneration and selectivity of the composite film-modified gold electrode were both excellent. Thus, the novel sensor we developed here could serve as a highly sensitive, rapid and reproducible probe for NADH detection. Moreover, the applicability of this sensor to the rapid diagnosing of NADH related diseases shows the great potential for practical application.

Acknowledgments

This work was supported by National Natural Science Foundation of China (81301293) and National Science and Technology Major Projects for “Major New Drugs Innovation and Development” (2014ZX09507008).

Appendix A. Supplementary material

Supplementary data associated with this article can be found in the online version at http://dx.doi.org/10.1016/j.bios.2015.02.031.

References

Alano, C.C., Ying, W., Swanson, R.A., 2004. J. Biol. Chem. 279, 18895–18902.
Banks, C.E., Davies, T.J., Wildgoose, G.G., Compton, R.G., 2005. Chem. Commun. 7, 829–841.
Bernofsky, C., Swan, M., 1973. Anal. Biochem. 53, 452–458.
Blaedel, W.J., Jenkins, R.A., 1975. Anal. Chem. 47, 1337–1343.
Cao, X., Ye, Y., Liu, S., 2011. Anal. Biochem. 417, 1–16.
Ding, B., Deng, Z., Yan, H., Cabrini, S., Zuckermann, R.N., Bokor, J., 2010. J. Am. Chem. Soc. 132, 3248–3249.
Geim, A.K., Novoselov, K.S., 2007. Nat. Mater. 6, 183–191.
Kasimova, M.R., Grigiene, J., Krab, K., Hagedorn, P.H., Flyvbjerg, H., Andersen, P.E., Møller, I.M., 2006. Plant Cell 18, 688–698.
Ke, Y., Lindsay, S., Chang, Y., Liu, Y., Yan, H., 2008. Science 319, 180–183.
Li, D., Muller, M.B., Gilje, S., Kaner, R.B., Wallace, G.G., 2008. Nat. Nanotechnol. 3, 101–105.
Li, J., Fan, C., Pei, H., Shi, J., Huang, Q., 2013a. Adv. Mater. 25, 4386–4396.
Li, L., Lu, H., Deng, L., 2013b. Talanta 113, 1–6.
Li, Z., Huang, Y., Chen, L., Qin, X., Huang, Z., Zhou, Y., Meng, Y., Li, J., Huang, S., Liu, Y., Wang, W., Xie, Q., Yao, S., 2013c. Sens. Actuators, B 181, 280–287.
Li, Z., Niu, T., Zhang, Z., Bi, S., 2010. Electrochim. Acta 55, 6907–6916.
Lin, W.J., Liao, C.S., Jhang, J.H., Tsai, Y.C., 2009. Electrochem. Commun. 11, 2153–2156.
Manesh, K.M., Santhosh, P., Gopalan, A., Lee, K.P., 2008. Talanta 75, 1307–1314.
Maune, H.T., Han, S.P., Barish, R.D., Bockrath, M., Iii, W.A., Rothemund, P.W., Winfree, E., 2010. Nat. Nanotechnol. 5, 61–66.
Moiroux, J., Elving, P.J., 1978. Anal. Chem. 50, 1056–1062.
Musameh, M., Wang, J., Merkoci, A., Lin, Y., 2002. Electrochem. Commun. 4, 743–746.
Nangreave, J., Han, D., Liu, Y., Yan, H., 2010. Curr. Opin. Chem. Biol. 14, 608–615.
Pal, S., Deng, Z., Ding, B., Yan, H., Liu, Y., 2010. Angew. Chem. Int. Ed. Engl. 49, 2700–2704.
Pei, H., Liang, L., Yao, G., Li, J., Huang, Q., Fan, C., 2012. Angew. Chem. 124, 9154–9158.
Pei, H., Lu, N., Wen, Y., Song, S., Liu, Y., Yan, H., Fan, C., 2010. Adv. Mater. 22, 4754–4758.
Pei, H., Zuo, X., Pan, D., Shi, J., Huang, Q., Fan, C., 2013. NPG Asia Mater. 5, e51.
Pumera, M., Scipioni, R., Iwai, H., Ohno, T., Miyahara, Y., Boero, M., 2009. Chem. Eur. J. 15, 10851–10856.
Renault, G., Raynal, E., Sinet, M., Berthier, J.P., Godard, B., Cornillault, J., 1982. Opt. Laser Technol. 14, 143–148.
Rinker, S., Ke, Y., Liu, Y., Chhabra, R., Yan, H., 2008. Nat. Nanotechnol. 3, 418–422.
Samec, Z., Elving, P.J., 1983. J. Electroanal. Chem. 144, 217–234.
Segal, M., 2009. Nat. Nanotechnol. 4, 612–614.
Shan, C., Yang, H., Han, D., Zhang, Q., Ivaska, A., Niu, L., 2010. Biosens. Bioelectron. 25, 1504–1508.
Shao, Y., Wang, J., Wu, H., Liu, J., Aksay, I.A., Lin, Y., 2010. Electroanalysis 22, 1027–1036.
Shim, J.H., Kim, J., Go, A., Lee, C., Lee, Y., 2013. Mater. Lett. 91, 330–333.
Su, W., Cho, M., Nam, J.D., Choe, W.S., Lee, Y., 2013. Electroanalysis 25, 380–386.
Teymourian, H., Salimi, A., Khezrian, S., 2013. Biosens. Bioelectron. 49, 1–8.
Tiwari, I., Gupta, M., 2014. Mater. Res. Bull. 49, 94–101.
Tkac, J., Davis, J.J., 2008. J. Electroanal. Chem. 621, 117–120.
Virag, L., Szabo, C., 2002. Pharmacol. Rev. 54, 375–429.
Voigt, N.V., Torring, T., Rotaru, A., Jacobsen, M.F., Ravnsbaek, J.B., Subramani, R., Mamdouh, W., Kjems, J., Mokhir, A., Besenbacher, F., Gothelf, K.V., 2010. Nat. Nanotechnol. 5, 200–203.
Vrecko, K., Storga, D., Birkmayer, J.G.D., Reinhard, M., Tafeit, E., Horejsi, R., Reibnegger, G., 1997. Biochim. Biophys. Acta 1361, 59–65.
Wen, Y., Pei, H., Wan, Y., Su, Y., Huang, Q., Song, S., Fan, C., 2011. Anal. Chem. 83, 7418–7423.
Wimpenny, J.W.T., Firth, A., 1972. J. Bacteriol. 111, 24–32.
Wu, L., Zhang, X., Ju, H., 2007. Anal. Chem. 79, 453–458.
Yates, S.P., Merrill, A.R., 2005. Anal. Biochem. 340, 41–51.
Ying, W., 2008. Antioxid. Redox Signal. 10, 179–206.
Yu, Q., Heikal, A.A., 2009. J. Photochem. Photobiol. B 95, 46–57.